

# In situ detection of monovalent copper in aerosols by photoemission

M. Ammann<sup>1</sup>, R. Hauert<sup>2</sup>, and H. Burtscher<sup>1</sup>

<sup>1</sup> Swiss Federal Institute of Technology, Solid State Physics, ETH Hönggerberg, CH-8093 Zürich, Switzerland

<sup>2</sup> Swiss Federal Laboratories for Materials Testing and Research, CH-8600 Dübendorf, Switzerland

Received November 6, 1991

**Summary.** In situ information on nanoparticle surface chemistry and modes of particle growth is obtained in gas suspension by the technique of photoelectric charging of particles (PCP) which depends on the surface chemical composition as well as the electronic structure of the particles via the spectral dependence of the photoelectric yield. With CuCl particles, photoelectric charging is about 100 times more efficient compared to other divalent transition metal compounds. Therefore, particles containing monovalent Cu can be detected with extremely high sensitivity of below 10 ng/m<sup>3</sup>. In atmospheric aerosols emitted from volcanoes, the relation of solid state oxidation/reduction in Fe<sub>1-x</sub>Cu<sub>x</sub>Cl<sub>2</sub> resulting in monovalent Cu for  $x < 0.4$  is important. As an example of the PCP technique this relation is monitored in laboratory generated aerosols. The nanoparticles are also precipitated onto a substrate where their surface chemical composition is analyzed by XPS which is important for the interpretation of the results obtained by photoelectric charging.

## 1 Introduction

Natural and anthropogenic sources emit about 30000 tons of particulate copper per year into the atmosphere [1]. About 70% are emitted as ultrafine aerosol particles in volcanic gases [2]. Field studies at different volcanoes have shown the fractionation of magmatic copper in volcanic gases [3] and its importance for volcano monitoring purposes [4]. Copper is emitted as a monovalent copper chloride and is embedded with an iron oxide in alkali chloride crystals in the nanometer size range. In long term exposure to the atmosphere of a volcanic plume containing SO<sub>2</sub> and H<sub>2</sub>SO<sub>4</sub>, the conversion of the chlorides into sulphates must be taken into account to understand the behaviour of copper containing aerosols in the atmosphere.

Ultrafine aerosol sampling in the field as well as in the laboratory requires extremely long sampling times to get enough material for standard chemical analysis. In addition sophisticated filters must be designed for the filtration of very small particles. Very often further chemical reactions on the filters cannot be excluded. Therefore in situ measurement

Offprint requests to: H. Burtscher

techniques are highly needed, offering the additional advantage of online analysis, which is not only fruitful in aerosol measurements in an atmospheric environment but also in controlling of nanoparticle processing in the field of material technology.

Up to now photoelectric charging of particles (PCP), also known as aerosol photoemission is the only in situ aerosol analysis technique being capable of both sensing the surface and the internal chemical structure of ultrafine particles [5]. The analytical potential of aerosol photoemission has previously been used to investigate oxygen adsorption on clean metal particles [6], coating of soot particles with organics [7] and the detection of heavy metal aerosols [8].

In this work, PCP is applied to some simple inorganic compounds of alkali and transition metal elements in view of applications with complex chemical structures of aerosol particles. Special emphasis will be on the detection of monovalent copper compounds. This will be applied to the monitoring of an relation of oxidation/reduction between Fe(II)/Cu(II) and Fe(III)/Cu(I) in small particles.

## 2 Aerosol generation

In order to produce aerosol particles of known chemical composition two common aerosol generation techniques have been applied [9]: 1) the gas evaporation technique in a tube furnace for volatile compounds being stable as gaseous molecules at elevated temperatures and 2) atomization in a solution nebulizer for water soluble materials.

### 2.1 Tube furnace

A carrier gas (filtered air or N<sub>2</sub>) is led over a sample of the desired material within a ceramic tube furnace. The temperature in the furnace can be adjusted between 100 and 1000°C. According to the temperature and the vapour pressure of the material, particles are formed in the carrier gas after the sample by homogeneous nucleation and condensation leading to a lognormal size distribution between 2 and 20 nm in radius. For this study aerosol particles of NaCl, KCl, MgCl<sub>2</sub>, CuCl, ZnCl<sub>2</sub>, FeCl<sub>2</sub>, PbBr<sub>2</sub> have been produced by this method. To avoid particle agglomeration the temperature was adjusted to give concentrations smaller than 10<sup>6</sup> particles per cm<sup>3</sup>.

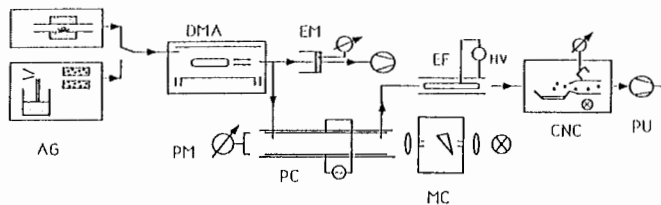


Fig. 1. Experimental setup for measurement of the photoelectric yield as function of particle size and photon energy. *AG* Aerosol generator; *DMA* Differential mobility analyzer; *EM* Electrometer; *PM* Photodetector; *PC* Photoemission chamber; *MC* Prism monochromator; *EF* Electrostatic precipitator; *CNC* Condensation Nucleus Counter; *PU* Pump

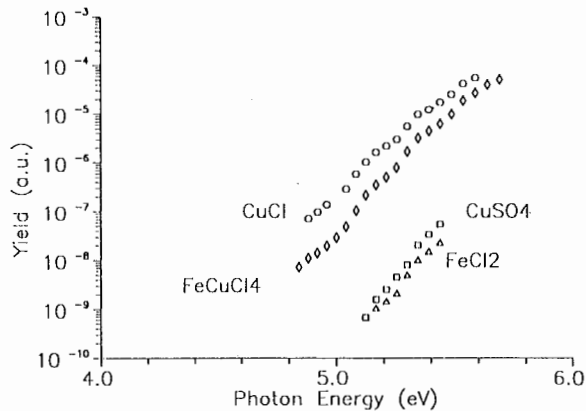


Fig. 2. Photoelectric yield (emitted electrons per incident photon) as function of the photon energy for aerosols consisting of CuCl, FeCuCl<sub>4</sub>, CuSO<sub>4</sub>, FeCl<sub>2</sub>. Equivalent mobility radii of the particles are 9.5 nm, 17 nm, 21 nm, 21 nm, respectively

## 2.2 Solution nebulizer

A solution containing a chloride or sulphate as solute is dispersed in a carrier gas into small droplets of some microns in diameter by a simple spray technique. In a diffusion dryer filled with silicagel the water evaporates leaving solid particles of the solute with radii between 5 and 50 nm. By this technique aerosols of Na<sub>2</sub>SO<sub>4</sub>, K<sub>2</sub>SO<sub>4</sub>, CuSO<sub>4</sub>, CuCl<sub>2</sub>, FeSO<sub>4</sub>, MgSO<sub>4</sub>, ZnSO<sub>4</sub> have been generated. Again the amount of solute is low enough to produce not more than 10<sup>6</sup> particles per cm<sup>3</sup>.

## 3 Aerosol analysis

### 3.1 Photoelectric charging of particles (PCP)

In PCP particles suspended in the carrier gas are irradiated with UV light of energy close to the photoelectric threshold. If the energy of the light is higher than the photoelectric threshold, electrons may be emitted from the particles, thus neutralizing particles with one initial negative charge or charging initially neutral particles positively. The photoelectric yield for light of energy  $E$  is defined as

$$Y = i_e / 4\pi R^2 j(E)$$

where  $i_e$  denotes the flux of emitted electrons per second,  $4\pi R^2$  the emitting surface area assuming a spherical particle of radius  $R$ , and  $j(E)$  the photon flux density at energy  $E$ . Within the light energy range of 4 to 10 eV and for particle radii below 50 nm the yield of photoelectrons is mainly deter-

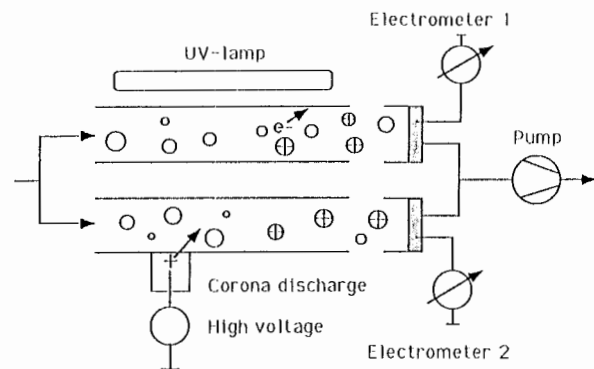


Fig. 3. Schematic diagram of the PCP probe. The photoelectric activity is determined by the quotient of the signals from electrometers 1 and 2. The flow rate is 66.7 cm<sup>3</sup>/s in each channel

mined by the escape probability of the excited electrons, justifying the use of  $4\pi R^2$  in the definition of the yield. The apparatus shown in Fig. 1 has been used to measure the photoelectric yield as function of the photon energy and the particle size. The differential mobility analyzer (DMA) [9] selects negatively charged particles of one electrical mobility from the polydisperse size spectrum produced by the aerosol generators described above. The so-called equivalent mobility radius  $R$  can be calculated from the electrical mobility [9]. The total gas flow rate of 66.7 cm<sup>3</sup>/s through the apparatus is provided by a pump. An electrometer measures the concentration of particles leaving the DMA. The intensity of the parallel UV light beam from a high pressure Xe/Hg lamp followed by a prism monochromator is measured with a photometer at the end of the photoemission chamber. There part of the initially negatively charged particles are neutralized by emission of photoelectrons. The highly mobile emitted electrons are removed by an alternating electric field in the photoemission chamber to prevent them from attachment to other particles. After electrostatic precipitation of the remaining negative particles in a cylindrical condenser, the neutral particles are counted with a condensation nucleus counter (CNC, TSI Model 3025) [9]. As long as the fraction of neutralized particles remains small (usually up to 1%), the signal of the CNC equals the amount of photoelectrons emitted in the photoemission chamber when neglecting particle losses to the wall within the apparatus. The photoelectric yield can be determined by dividing the CNC signal through the light intensity, the particle concentration and  $4\pi R^2$ . As an example, Fig. 2 shows the photoelectric yield of aerosols of some transition metal compounds as function of the incident light energy.

Much higher sensitivity at a fixed light energy is obtained with an even simpler apparatus. Designed as a compact probe, it can be used in the laboratory as well as in the field [10] (Fig. 3). The increase in sensitivity is achieved by giving up the size selectivity and by using a low pressure mercury lamp with an intense line at 6.7 eV without a monochromator. In this case initially neutral particles are charged in the photoemission chamber due to electron emission upon UV irradiation. To obtain a measure for the surface area  $4\pi R^2$  of the particles, the flow of neutral particles is split into two parts, one passing the photoemission chamber, the other going through an ion attachment unit, where positive ions are produced by an electric corona discharge. For spherical

**Table 1.** Photoelectric activity  $\epsilon$  (measured at 6.7 eV) for aerosols of various inorganic salts

Compound	$\epsilon$	Exp.
(NH <sub>4</sub> ) <sub>2</sub> SO <sub>4</sub>	0	s
NaCl	0	f,s
Na <sub>2</sub> SO <sub>4</sub>	0	s
MgCl <sub>2</sub>	0	s
KCl	0	f,s
K <sub>2</sub> SO <sub>4</sub>	0	s
CaCl <sub>2</sub>	0	s
FeCl <sub>2</sub>	0.05	f,s
FeSO <sub>4</sub>	0.02	s
CuCl	0.9	f
CuCl <sub>2</sub>	0.02	s
CuSO <sub>4</sub>	0.02	s
ZnCl <sub>2</sub>	0	f,s
ZnSO <sub>4</sub>	0	s
SnCl <sub>2</sub>	0.04	s
PbBr <sub>2</sub>	0.02	f

'f' and 's' denote particle generation with tube furnace and solution nebulizer, respectively

particles with radii below 100 nm the charge acquired in the latter is proportional to the surface area  $4\pi R^2$  but is independent of the material. After removal of remaining ions in the gas by a weak electric field, the flux of charged particles is measured with electrometers. The ratio of the charges in the two channels is called photoelectric activity  $\epsilon$ . As the photoelectric charge depends on the light intensity of the lamp, the intensity is monitored in all experiments to offer the possibility of new calibration in case of changes. This ensures reproducible operating conditions. Thus, dividing the photoelectric charges by the surface area gives photoelectric activity  $\epsilon$  as a normalized quantity which is proportional to the photoelectric yield at 6.7 eV. On the one hand,  $\epsilon$  is dependent on the shape of the photoelectric yield curve which is more or less a material constant. On the other hand,  $\epsilon$  depends on the photoelectric threshold, which is a function of the electronic structure of the material and of the surface of the aerosol particles as well (geometry, adsorbed surface layers). Assuming that in most transition metal compounds the density of states close to the vacuum level is largely constant so that light absorption in the range of 4 to 10 eV is not a strong function of the photon energy, the yield curve for a material (see for example Fig. 2) shifts parallel along the energy axis, when the threshold is shifted by changes on the particle surface.

With the described experimental setup, the values of  $\epsilon$  range from  $10^{-4}$  up to 10. Limitations are imposed by small ion attachment coefficients for very small particles, the sensitivity of the electrometer ( $10^{-15}$  A) and multiple photoemission charging effects for particles with very high photoelectric activity.

### 3.2 X-ray photoelectron spectroscopy (XPS-ESCA)

In order to get more complete chemical information on the surface of the particles, aerosol samples are further investigated by XPS.

Sampling is achieved as follows: neutral particles are charged by ion attachment and then precipitated electrostatically on a HOPG surface (highly oriented pyrolytic

graphite). A monolayer of particles (enough for analysis) on the substrate requires sampling times of the order of 1 h for particles 10 nm in radius and  $10^6$  cm<sup>-3</sup> concentration. To prevent the samples from oxidation they are kept in a noble gas environment until transfer into the XPS apparatus.

In XPS the surface under investigation is irradiated by monoenergetic X-rays (Mg-K $\alpha$  radiation at  $h\nu = 1253.6$  eV). The energy spectrum of the emitted photoelectrons provides an image of the binding energies of the core electrons from the elements present at the surface. The small deviations of the peak positions namely the chemical shifts, reveal the valence state or the chemical environment of the different elements involved. The analyzed depth is determined by the inelastic mean free path of the excited electrons and ranges from 1 to 3 nm.

XPS measurements were carried out on a Perkin Elmer PHI 5400 ESCA system. The electron energy analyzer was operated at a constant pass energy of 35.36 eV, the total energy resolution being 0.89 eV (Ag 3d<sub>3/2</sub>), analyzing an area of 1.1 mm in diameter. The binding energy scale was calibrated for the Au 4f<sub>7/2</sub> signal at  $83.8 \pm 0.1$  eV. The base pressure was  $4 \times 10^{-10}$  mbar. Further details concerning surface analysis by XPS-ESCA can be found in the book of Briggs and Seah [11].

## 4 Results and discussion

### 4.1 Photoelectric activity of CuCl

As stated above the photoelectric activity  $\epsilon$  provides a general parameter sensing the surface of the particles as well as the chemical composition. To get an overall picture of the possible analytical capability of this method  $\epsilon$  was measured for a number of alkali, alkali earth and transition metal compounds as aerosol particles suspended in air. The results are summarized in Table 1. As the ionization potential of alkali chlorides is higher than 8 eV [12], the photoelectric activity of KCl, NaCl, K<sub>2</sub>SO<sub>4</sub>, Na<sub>2</sub>SO<sub>4</sub> measured at 6.7 eV is zero. For the same reason  $\epsilon$  is zero for MgCl<sub>2</sub> and CaCl<sub>2</sub> as well as for ZnCl<sub>2</sub>, which has an ionization energy of 12.9 eV [13].  $\epsilon$  values of the order of  $10^{-2}$  are found for the group IV dihalides of Pb and Sn. The same order of magnitude has been obtained from the transition metal dihalides and sulphates of Cu and Fe, whereas the photoelectric activity of the monovalent CuCl is by orders of magnitudes higher which may also be inferred from Fig. 2. This figure shows that the photoelectric threshold (i.e. the onset of photoemission) for the investigated iron and copper compounds lies below 5 eV. This relatively low threshold (a clean CuCl surface has a photoelectric threshold of 6.8 eV [14]) is due to the formation of an oxide layer on the surface of the particles after exposure to ambient air. A similar behaviour of the photoelectric threshold after oxygen exposure is also observed in Ni metal particles [15] when the oxide forms on the surface. Figure 4 shows the XPS spectrum of CuCl particles with the fourfold splitted 2 p line indicating the presence of Cu(II) ions on the particle surface (monovalent Cu(I) reveals only a twofold splitted 2 p line). The large difference in photoelectric activity  $\epsilon$  between the monovalent and the divalent copper compounds is mainly due to the difference in the photoelectric yield. This effect can be used to detect monovalent copper ions among other compounds within small aerosol particles with high sensitivity. The detection limit of the electrometers used in

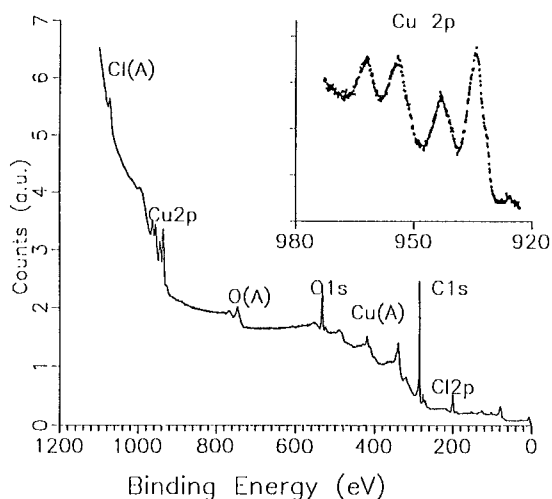


Fig. 4. XPS-spectrum of CuCl aerosols precipitated on HOPG substrate (as deposited). A denote lines from Auger transitions. Inset: Cu 2p line with characteristic satellite structure of Cu(II)

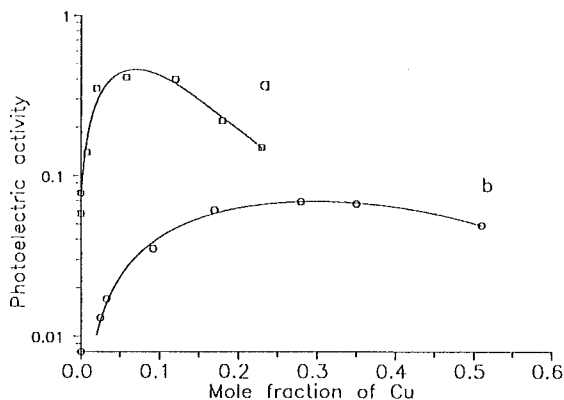


Fig. 5. Photoelectric activity  $\epsilon$  as function of Cu mole fraction in mixed sodium-iron chloride (a) and sulphate (b) aerosols. Fe/Na = 0.099 in (a) and Fe/Na = 0.18 in (b)

the instrument (Fig. 3) is below  $10^{-15}$  A. When working with flow rates of  $66.7 \text{ cm}^3/\text{s}$  this corresponds to a charge concentration of  $10^2$  charges per  $\text{cm}^3$ . The ion attachment efficiencies are of the order of 20% for particles with radii of 10 nm [9],  $\epsilon$  being close to 1. A CuCl particle concentration of less than  $10^3 \text{ cm}^{-3}$  can produce still measurable currents in both electrometers. The sensitivity for an in situ measurement of CuCl as aerosols is thus of the order of  $10 \text{ ng}/\text{m}^3$  corresponding to a mass flux of 0.04 ng per minute.

The relationship between the CuCl mass concentration of a pure CuCl aerosol and the photoemission charging rate has not been investigated systematically, but in all the experiments the photoelectric activity of CuCl for different sizes and concentrations was the same (deviations have never been larger than 5%). Thus the photoemission charging rate increases linearly with increasing particle surface area.

PCP may be used when monovalent copper must be detected among other divalent transition metal compounds in similar amounts. In mixtures with materials with very high photoelectric thresholds, for example when CuCl is embedded in NaCl crystals, part of the photoelectrons may be absorbed by the NaCl, and probably the photoelectric

threshold of the particles is a function of the relative CuCl content, thus giving rise to an underestimation of the CuCl content.

The high photoelectric yield of CuCl is in agreement with the work of Krolkowski [16], where normalized yield data are available for bulk CuI, and with the yield of CuBr reported by Lin et al. [17]. Goldmann [14] discussed the electronic structure of the tetrahedrally coordinated cuprous halides. The key feature seems to be the partial ligand p admixture to the copper 3d bands. The partial p and d densities of states near the top of the valence band, from where electrons in UV photoemission are excited, could be determined only with limited accuracy in the work of Goldmann [18].

The only PCP measurement of a monovalent copper compound is reported by Niessner et al. [8], where  $\text{Cu}_2\text{O}$  particles were analyzed with an aerosol photoemission sensor array with different UV irradiation wavelengths (185, 214, 229, 254 nm). The  $\text{Cu}_2\text{O}$  particles could be charged photoelectrically at all light energies, whereas none of the energies was high enough to ionize particles of CuO, in agreement with our findings of the difference in photoelectric activity between the monovalent and the divalent copper compound.

#### 4.2 Copper valence in mixed iron copper chloride aerosols

In experiments with different salt mixtures from the solution nebulizer an enhancement of photoelectric activity  $\epsilon$  has been observed when divalent iron and copper salts are used together. Referring to the measurements summarized in Table 1 this enhancement is supposed to be due to a reduction of the divalent copper ions. In the experiment summarized in Fig. 5 the initial solution in the solution nebulizer contained 91%  $\text{Na}^+$  and 9%  $\text{Fe}^{2+}$  as cations and  $\text{Cl}^-$  as anion (Fig. 5a) before different amounts of  $\text{CuCl}_2$  have been added. In the same way sulphate solutions have been prepared starting with 85%  $\text{Na}^+$  and 15%  $\text{Fe}^{2+}$  and adding  $\text{CuSO}_4$  (Fig. 5b). The photoelectric activity  $\epsilon$  of the resulting particles is plotted against the relative fraction of Cu ions in the aerosols. In both cases a distinct maximum is observed when the Cu fraction is in the order of the Fe(II) fraction, the height of the maximum indicating almost complete reduction of Cu(II) to Cu(I).

To get more defined conditions, the experiment has been repeated without using a sodium chloride matrix and by working with the experimental setup shown in Fig. 1. As discussed in the previous section,  $\epsilon$  is related to the photoelectric yield at 6.7 eV. Figure 6 shows the relative photoelectric yield at 5.4 eV of  $\text{Cu}_x\text{Fe}_{1-x}\text{Cl}_2$  particles with radii of 17 nm measured as function of  $x$  in filtered air as carrier gas. Again a marked maximum in the yield is measured for  $x = 0.4$ . The yield for  $x = 1$  lies below the detection limit of the apparatus which is identical with the lower limit of the scale in Fig. 6. In order to get evidence of the supposed reduction of the divalent copper due to the presence of divalent iron, samples of aerosols with  $x = 0$ ,  $x = 0.3$ ,  $x = 0.9$  and  $x = 1$  have been analysed by XPS. The relevant  $\text{Cu}_{2p}$  and  $\text{Fe}_{2p}$  lines of the XPS spectrum are presented in Fig. 7a and b, respectively. Up to Cu fractions corresponding to the maximum of Fig. 6 the only twofold splitted line (Fig. 7a,  $x = 0.3$ ) indicates complete reduction to Cu(I) whereas for larger fractions (Fig. 7a,  $x = 0.9$  and  $x = 1$ ) the fourfold splitted part of the line increases showing the partial oxida-

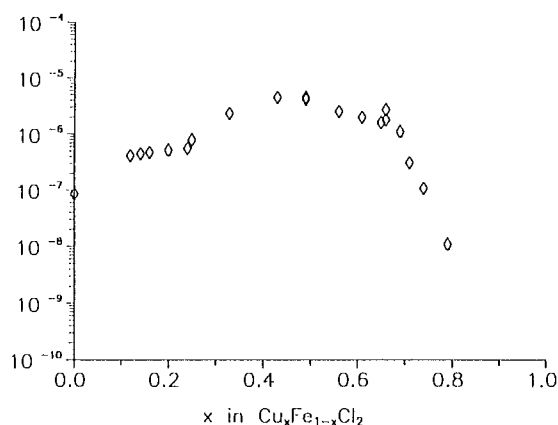


Fig. 6. Relative photoelectric yield at 5.39 eV as function of the Cu fraction  $x$  in  $\text{Cu}_x\text{Fe}_{1-x}\text{Cl}_2$  particles suspended in air

tion, according to the relative amount of Fe(II) in the particles. In the same time the  $\text{Fe}_{2p}$  line shifts from the Fe(II) position (710.4 eV) for  $x = 0$  to the Fe(III) position (711.2 eV) for complete oxidation at  $x = 0.9$ . Clearly partial oxidation can be seen for  $x = 0.3$ . Thus the PCP measurement contains already the complete information on the distribution of Cu(I) and Cu(II) in the aerosol particles.

The standard reduction potentials [West et al. 1984] do not allow such a redox process to occur in aqueous solutions. A solid state reaction within the aerosol particles is assumed similar to that described by D'Huysser et al. [19] for bulk copper ferrites. The maximum in Fig. 6 near  $x = 0.4$  indicates reduction of Cu(II) by two thirds of the Fe(II) ions present in the particles, pointing probably to different coordination sites of the ions in analogy to the copper ferrites.

Being sensitive to the sample surface only, XPS shows that Cu(I) is not oxidized on the particle surface by exposure to ambient air as it occurs in pure CuCl particles (Fig. 4). Thus the reduction oxidation equilibrium between iron and copper ions has an important implication for the measurement of atmospheric aerosol particles in the vicinity of volcanoes: in the volcanic gas copper is condensing as a monovalent compound which is not oxidized in ambient air due to the presence of iron oxides within the particles.

## 5 Conclusions

Photoelectric charging of particles (PCP), an extremely sensitive in situ aerosol analytic tool, has been applied to alkali and transition metal chlorides and sulphates. The most striking feature is the very high photoelectric yield of particles consisting of monovalent copper compounds, compared to the divalent compounds of copper and iron. With pure CuCl particles, XPS on precipitated particles reveals the oxidized surface layer lowering the photoelectric threshold. This lowering of the photoelectric threshold combined with the sharp increase of the intrinsic photoelectric yield of CuCl explains the high photoelectric activity, which is proportional to the yield at 6.7 eV. PCP therefore allows the in situ detection of fine CuCl aerosol particles in the nanometer size range in concentrations below  $10 \text{ ngm}^{-3}$ . As an application a solid state redox reaction of Cu(II)/Fe(II) has been monitored in  $\text{Fe}_{1-x}\text{Cu}_x\text{Cl}_2$  particles as well as in alkali salt particles containing traces of Fe and

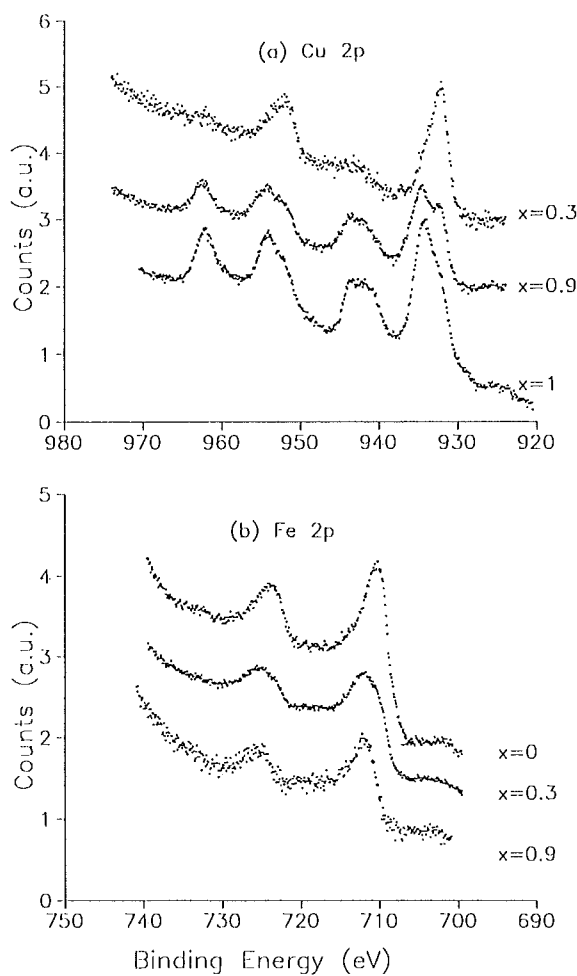


Fig. 7. Cu 2p (a) and Fe 2p (b) lines from XPS spectra as deposited of samples of  $\text{Cu}_x\text{Fe}_{1-x}\text{Cl}_2$  particles for various Cu fractions  $x$

Cu ions. For  $x < 0.4$ , Cu is only present as Cu(I), even at the surface of the particles, as shown by the XPS spectra.

This redox equilibrium preserves the monovalent copper ions in the aerosol particles from oxidation in ambient air under the condition that enough iron is present. PCP is now successfully applied in field measurements at a volcano for monitoring the particulate copper emissions in the volcanic gas.

In conclusion, quantitative determination of copper valence in complex nanoparticle systems is not out of sight. Beside its relevance in volcanic aerosols, possible applications in the field of superconducting materials should be discussed, where the valence of copper plays a crucial role.

*Acknowledgement.* We are grateful to L. Scherrer for his technical support and the development of the PCP probe. We thank Prof. H. C. Siegmann for his contribution to this project and the many fruitful discussions.

## References

1. Nriagu JO, Pacyna JM (1988) *Nature* 333:134–139
2. Le Cloarec M-F, Marty B (1991) *Terra Nova* 3:17–27
3. Pennisi G, Le Cloarec M-F, Lambert G, Le Rouilly JC (1988) *Earth Planet Sci Lett* 88:284–288
4. Ammann M, Hauert R, Burtscher H, Siegmann HC (1991) submitted to *J Geophys Res*

5. Bartscher H, Scherrer L, Siegmann HC, Schmidt-Ott A, Federer B (1982) *J Appl Phys* 53:3787–3791
6. Müller U, Schmidt-Ott A, Bartscher H (1987) *Phys Rev Lett* 58:1684–1686
7. Bartscher H, Schmidt-Ott A (1986) *J Aerosol Sci* 17:669–703
8. Niessner R, Hemmerich B, Panne U (1989) *Fresenius Z. Anal Chem* 335:728–737
9. Hidy GM (1984) *Aerosols, An Industrial and Environmental Science*. Academic Press, Orlando
10. Ammann M, Bartscher H (1990) *Bull Volcanol* 52:577–583
11. Briggs D, Seah MP (1990) *Practical surface analysis*. Wiley, New York
12. Weast RC, Astle MJ, Beyer WH (1984) *Handbook of chemistry and physics*. CRC Press, Boca Raton
13. Bailar JC (1973) *Comprehensive inorganic chemistry*. Pergamon Press, Oxford
14. Goldmann A (1974) *Phys Stat Sol* 81:9–47
15. Müller U, Ammann M, Bartscher H, Schmidt-Ott A (1991) *Phys Rev B* 44:8284–8287
16. Krolikowski WF (1967) Ph D Thesis Stanford Electronics Laboratories
17. Lin SF, Spicer WE (1976) *Phys Rev B* 14:4551–4558
18. Goldmann A, Tejada J, Shevchik NJ, Cardona M (1974) *Phys Rev B* 10:4388–4402
19. D'Huysser A, Lerebours-Hannoyer B, Lenglet M, Bonnelle J-P (1981) *J Solid State Chem* 39:246–256